

The Salinity, Heat, and Buoyancy Budgets of a Coastal Current in a Marginal Sea

A. K. WÄHLIN

Earth Sciences Center, University of Gothenburg, Göteborg, Sweden

H. L. JOHNSON

Department of Earth Sciences, University of Oxford, Oxford, United Kingdom

(Manuscript received 8 July 2008, in final form 7 April 2009)

ABSTRACT

The Atlantic overturning circulation has conventionally been pictured in the meridional-vertical plane, but a significant densification of the water masses involved also occurs as the surface branch of the circulation flows in boundary currents around the subpolar gyre and northern marginal seas. Here an analytical model of the heat and salt budget for an idealized coastal boundary current in a marginal sea is presented. The boundary current exchanges heat and freshwater with the atmosphere as well as with the interior of the basin through eddy and Ekman transports. Its along-coast volume transport is assumed to be constant and independent of buoyancy; it is set, for example, by the wind forcing. Because the atmospheric fluxes of heat and freshwater are different, the temperature and salinity of the boundary current adjust on different length scales. The size of these length scales compared with the circumference of the basin determines the properties of the water that flows over the sill. Furthermore, the relative size of the two length scales determines the evolution of the density as the current moves around the basin. If temperature and salinity adjust on the same length scale (or if the density forcing is represented by a single component), then the density will increase or decrease monotonically from the inflow to the outflow. However, when the adjustment length scale for temperature is shorter than that for salinity, a warm and salty inflow can cool significantly before it freshens. As a result, the density first increases to a local maximum before decreasing again. Therefore, when salinity as well as temperature is included in the buoyancy forcing, the outflow from the basin can be significantly denser than for the equivalent single-component density forcing and can be more sensitive to the forcing parameters. The relevance and implications for the Nordic Seas are discussed.

AU1

1. Introduction

A boundary current that interacts with the atmosphere may transport heat and salt, and hence buoyancy, across latitude circles. Such transport is not necessarily linked to a large-scale sinking of the water mass (i.e., to the strength of a meridionally averaged overturning circulation). For example, a coastal boundary current flowing horizontally around a closed basin may not have any significant net vertical overturning associated with it, but it can still transport heat into the basin and give rise to significant ocean buoyancy loss.

The concept of a large-scale thermohaline circulation taking place in horizontal gyres in a marginal sea was

explored by Mauritzen (1996a,b). Mauritzen showed, based on observations, that the dense water that feeds the Denmark Straits overflow consists of Atlantic surface water that has been modified during a horizontal loop along the topography in the Nordic Seas and Arctic Ocean (see also Isachsen et al. 2007). The dense water thus produced ventilates the deep Atlantic Ocean and plays a key role in the Atlantic meridional overturning circulation, with an associated northward heat transport that helps to maintain European climate (Vellinga and Wood 2002). The sensitivity of the dense water formation process to anthropogenic climate change is as yet unclear (Solomon et al. 2007).

Spall (2002, 2003, 2004) examined the dynamics of water mass transformation in a series of idealized numerical experiments of a marginal sea subject to surface cooling. The warm inflow was found to flow cyclonically around the basin as a coastally trapped boundary or “rim” current, with much weaker motions in the interior.

Corresponding author address: A. K. Wåhlin, Earth Sciences Center, University of Gothenburg, Box 460, SE-405 30 Göteborg, Sweden.

E-mail: awahlin@gu.se

DOI: 10.1175/2009JPO4090.1

© 2009 American Meteorological Society

jpo4090

Water in the interior of the basin loses heat to the atmosphere and gains heat through eddy interactions with the rim current, whereas the current itself loses heat to both the atmosphere and the interior. Although there is some vertical circulation, mainly confined to the sloping boundaries (Spall 2003), the dominant buoyancy loss takes place in the horizontal gyre rather than in the vertical overturning circulation.

The forcing in Spall (2004) consisted of a spatially uniform but seasonally varying surface heat flux. An alternative surface boundary condition was applied to an otherwise similar setup in Walin et al. (2004), where a heat flux proportional to the difference between the surface temperature and a constant equilibrium temperature was applied (i.e., a relaxation condition on temperature). The main focus of that study was the transformation of the inflowing baroclinic current to a barotropic shelf current, but the numerical results are in many ways similar to those of Spall (2004). For example, the buoyant boundary current loses heat to the atmosphere and exchanges fluid via eddies with the basin interior. Walin et al. (2004) also note that the boundary current is always slightly warmer than the basin water, regardless of the strength of eddy exchange, the initial conditions, and the relaxation temperature. This is a natural consequence of the boundary condition: the basin water is essentially motionless and has reached the atmospheric relaxation temperature, whereas the rim current has heat added outside the basin and is still cooling when it exits.

The gradual densification of a boundary current as a result of eddy exchange with a convecting, dense interior was examined in an analytical model by Straneo (2006). Motivated primarily by the Labrador Sea, in which the Atlantic layer enters the basin well below the surface, direct heat loss from the boundary current to the atmosphere was neglected, and separate budgets for the boundary current and the basin interior were formulated. Heat lost from the inflowing boundary current was assumed to be transferred via eddies to the basin interior, from whence it is lost to the atmosphere.

The aim of the present study is to investigate the different effects of surface heat and freshwater fluxes on the density evolution of the boundary current. Allowing the boundary current to exchange buoyancy directly with the atmosphere is crucial in marginal seas such as the Nordic Seas, where the boundary current enters at the surface. The surface heat flux depends strongly on the sea surface temperature, whereas the salt flux arising from the freshwater input is much more weakly dependent on the surface salinity. As a consequence, salinity generally adjusts on a longer length scale than temperature. We examine the effect this has on the along-coast

development of density using an idealized analytical model. Unlike previous studies (Spall 2004; Straneo 2006; Walin et al. 2004), we assume that the volume exchange with the basin interior, as well as the along-coast transport in the boundary current, is constant. Our focus is not on the dynamics governing the flow but rather on the processes that determine the steady-state temperature, salinity, and density of the boundary current, averaged in the vertical and cross-stream directions.

In a model that represents density with a single component (temperature or salinity), the density adjustment along the path of the boundary current can only be monotonic (as in Spall 2004, Walin et al. 2004, and Straneo 2006). Here we show that when a two-component density is included, it is possible for the boundary current to reach a local maximum in density before it exits the basin. For this to happen, the adjustment length scale for temperature must be shorter than that for salinity. A warm and salty inflow will then cool faster than it freshens, and the water first becomes cool and salty before the salinity adjusts and the current becomes fresher and lighter. As a result, the outflow from the basin may be significantly denser than expected from the equivalent single-component density forcing, and can also be more sensitive to the forcing parameters. It is even possible to form water that is denser than the basin interior, so that the boundary current subducts beneath the surface. This cannot occur in single-component density systems or in systems where the adjustment length scales for salinity and temperature are equal (e.g., those in which the boundary current density is dominated by the exchange with the interior).

The paper is structured as follows: The salinity and heat budgets are outlined in section 2. In section 3 the buoyancy budget is formulated and discussed. Section 4 considers the relevance of this model to the Nordic Seas, and the results and conclusions are discussed in section 5.

2. Freshwater and heat budgets

Consider the buoyant coastal boundary current illustrated schematically in Fig. 1, which flows around the perimeter of an enclosed basin. Its along-coast volume transport Q may be set by the wind (either locally through Ekman effects or nonlocally outside the basin) or by other forces but is assumed to be constant throughout the basin and to be independent of the buoyancy loss. As a boundary current loses buoyancy along its path, the speed of the geostrophic current at the surface front decreases, along with the baroclinic transport associated with it. This decrease can be compensated either by a downwelling along the boundary (Straneo 2006) or by a transfer of water from the baroclinic core to a barotropic

F1

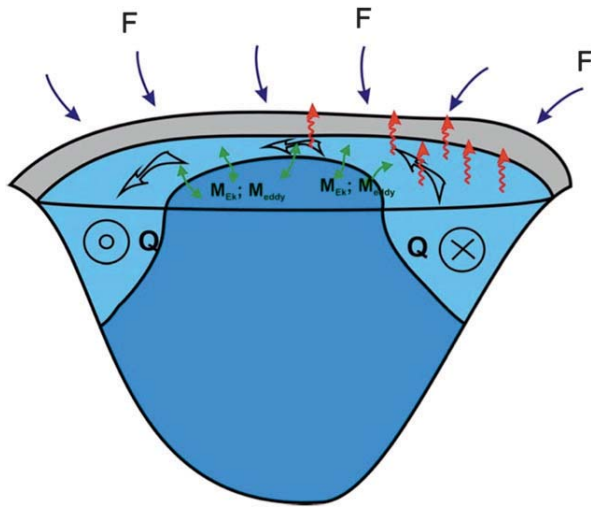


FIG. 1. Schematic view of a buoyant coastal boundary current with volume transport Q flowing around the perimeter of a marginal sea. The current exchanges water with the interior, exchanges heat with the atmosphere, and gains fresh water through runoff and precipitation.

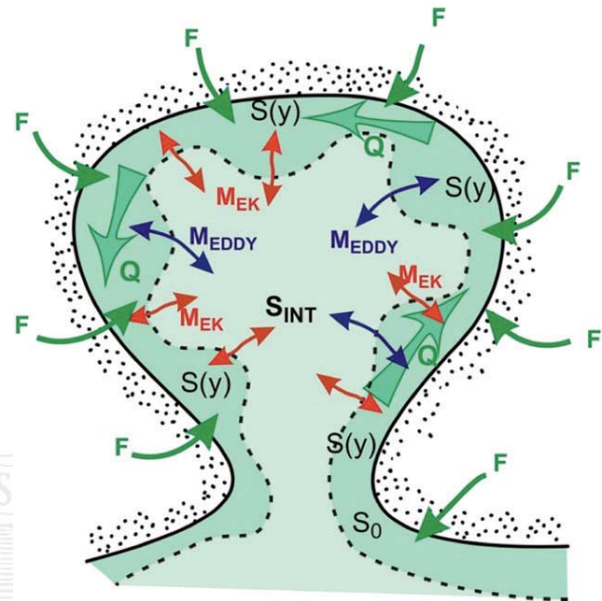


FIG. 2. Salinity budget of the boundary current.

core closer to the coast (Walín et al. 2004), in which case the total volume transport of the boundary current remains constant. Mass conservation in the marginal sea, combined with the assumption that all the flow exchanged between the basin and the adjacent ocean occurs on the boundary, also requires the transport of the boundary current to be constant (e.g., Spall 2004).

The boundary current in Fig. 1 has a constant width R and a path length L_B (equal to the perimeter length of the marginal sea) and is assumed to be well mixed in the vertical and across-current directions. It exchanges heat and freshwater directly with the atmosphere and the land. It also exchanges fluid with the interior at a rate $M = M_{\text{EDDY}} + M_{\text{EK}}$ ($\text{m}^2 \text{s}^{-1}$), through an eddy-induced volume exchange M_{EDDY} and a wind-driven Ekman exchange M_{EK} . Neither M_{EK} nor M_{EDDY} gives any net transport into the boundary current. If the dominant wind stress pattern is cyclonic, the surface Ekman transport is everywhere directed toward the boundaries with a return flow at depth. This is the case, for example, in the Nordic Seas (e.g., Furevik and Nilsen 2005). The eddy exchange M_{EDDY} varies in reality and depends on the eddy-creating mechanism. Cessi (2008) showed that a parameterization based on the kinetic energy balance of baroclinic eddies compares well with eddy-resolving models, whereas in Spall (2004) and Straneo (2006) the eddy exchange is assumed to increase linearly with the boundary current velocity (or equivalently the isopycnal slope). We might therefore expect M_{EDDY} to decrease as the density difference between the basin interior and

the boundary current decreases around the basin. However, since M_{EK} is independent of the density difference and (for the Nordic Seas) comparable in size to M_{EDDY} , and since our goal here is to study the different contributions of temperature and salinity adjustment within the boundary current to the density change, we treat M as a constant. This would of course not be justified if our aim were to establish what sets the boundary current strength (e.g., as in Straneo 2006), but is appropriate for the simple budget model developed here. In section 5 we show that for the Nordic Seas, the uncertainty in M results in a relatively small uncertainty in the outflow density compared to the uncertainty in the other parameters involved.

The buoyancy of the boundary current after modification by the exchanges with the interior, atmosphere, and land will determine whether it sinks (and if so to what depth) once it has left the marginal sea and entered the adjacent ocean. Although, by construction, no overturning takes place within the marginal sea itself, the temperature, salinity, and buoyancy at the outflow from the basin are crucial in determining the role that the marginal sea will play in the large-scale overturning circulation. We start by considering the freshwater and heat budgets of the boundary current separately before combining them to look at the density budget.

a. The freshwater budget

Figure 2 shows a sketch of the boundary current and the processes that determine its salinity. Freshwater is

FIG 2

added at a constant rate F ($\text{m}^2 \text{s}^{-1}$) per unit length of the boundary current by coastal runoff and precipitation and from low-salinity currents carrying freshwater along the coast. There is also an exchange $M = M_{\text{EDDY}} + M_{\text{EK}}$ ($\text{m}^2 \text{s}^{-1}$) of water with the interior of the basin, where the salinity is S_{INT} . The steady-state salinity budget of the boundary current is therefore given by

$$Q \frac{dS}{dy} = -M(S - S_{\text{INT}}) - FS, \quad (1)$$

where Q is the boundary current transport, y is the along-current coordinate, S is the mean (temporal, cross-current, and vertical) of the boundary current salinity, and $S = S_0$ at the inflow (i.e., at $y = 0$). Equation (1) can also be written

$$\frac{dS}{dy} = -\frac{S}{L_S} + \frac{S_{\text{INT}}}{L_E}, \quad (2)$$

where

$$L_S = \frac{Q}{F + M} \quad \text{and} \quad L_E = \frac{Q}{M} \quad (3)$$

are the relevant length scales of the problem. The solution to (2) is

$$\delta S(y) = \delta S_0 e^{-y/L_S}, \quad (4)$$

where

$$\delta S = S - S_{\text{EQ}}, \quad \delta S_0 = S_0 - S_{\text{EQ}}, \quad \text{and} \quad S_{\text{EQ}} = S_{\text{INT}} \frac{L_S}{L_E} = S_{\text{INT}} \left(\frac{1}{1 + F/M} \right). \quad (5)$$

Equation (4) describes an exponential adjustment on the length scale L_S of the initial salinity toward S_{EQ} . The value S_{EQ} , or the ‘‘equilibrium salinity’’, is the salinity at which the influence of freshwater forcing is precisely balanced by the exchange with the interior. It is the salinity that the boundary current would attain if it were fully adjusted to surface forcing by the time it left the basin. When F/M is small $S_{\text{EQ}} \approx S_{\text{INT}}$; but for larger values of F/M , S_{EQ} is significantly less than the interior salinity. It is independent of both S_0 and the volume transport Q .

The adjustment length scale L_S increases with Q and decreases with both F and M , reflecting the fact that a large boundary current with small exchanges with the basin interior and/or the atmosphere takes longer to reach equilibrium salinity. Whether the salinity reaches S_{EQ} before it exits the basin depends on the relative size of L_S and the length of the boundary current, L_B . When

$L_B/L_S \gg 1$, the basin is well adjusted in terms of salinity, $S_{\text{OUT}} = S_{\text{EQ}}$, and the salinity of the inflow is irrelevant ($\partial S_{\text{OUT}}/\partial S_0 = 0$). However, when $L_B/L_S < 1$ the equilibrium value is not reached and S_{OUT} also depends on S_0 .

The volume transport of the boundary current, Q , plays a role in determining which of these regimes the basin falls into, since it determines the length scale L_S . Note that S_{OUT} is most sensitive to changes in Q when $Q = 0.5L_B(F + M)$, or equivalently when $L_B/L_S = 2$, which roughly marks the transition between regimes of well-adjusted and nonadjusted outflow. This can be seen by setting the second derivative of Eq. (4) with respect to Q to zero at $y = L_B$. A change in the volume transport of the boundary current may therefore significantly affect the sensitivity of the outflow to the inflow salinity.

The salinity of the boundary current may either increase or decrease with y as it adjusts. If the boundary current is initially fresher than the basin interior ($S_0 < S_{\text{INT}}$), the exchange with the interior will add salt to the boundary current. However, this will be counteracted by a positive freshwater flux. There will be a net salinity increase only if $S_0 < S_{\text{EQ}}$, that is, if $F < M[(S_{\text{INT}}/S_0) - 1]$. For the special case $S_0 = S_{\text{EQ}}$, the salinity of the boundary current does not change.

b. The heat budget

Figure 3 shows a sketch of a small segment of the boundary current together with the processes that affect the temperature in that segment. A steady-state heat budget for the segment (see appendix A) can be expressed in the form

$$Q \frac{dT}{dy} = -R\gamma_A(T - T_{\text{AIR}}) - M(T - T_{\text{INT}}), \quad (6)$$

where R is the width of the boundary current, γ_A (m s^{-1}) is the temperature relaxation coefficient (see, e.g., Haney 1971), T_{AIR} is the air temperature (assumed constant in time and space) to which the boundary current temperature relaxes, T_{INT} is the temperature of the interior of the basin, and $T = T_0$ at the inflow (i.e., at $y = 0$). It was argued in Haney (1971) that a relaxation condition is most appropriate for modeling surface heat fluxes, and this is commonly used in numerical models and analytical box models. The use of a temperature relaxation condition rather than an imposed heat flux (as in Spall 2004) induces a spatial adjustment of the (steady) temperature along the path of the boundary current toward a constant equilibrium.

Equation (6) can also be written

$$\frac{dT}{dy} = -\frac{(T - T_{\text{AIR}})}{L_A} - \frac{(T - T_{\text{INT}})}{L_E}, \quad (7)$$

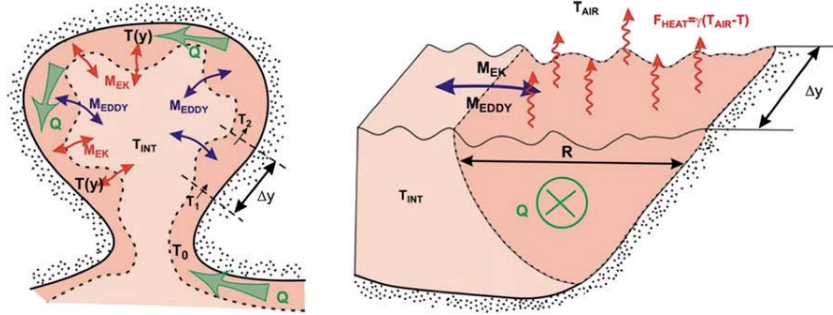


FIG. 3. Heat budget of a segment of the boundary current.

where $L_E = Q/M$ as before and where

$$L_A = \frac{Q}{R\gamma_A} \quad (8)$$

is the length scale imposed by the atmospheric forcing. The solution is given by

$$\delta T(y) = \delta T_0 e^{-y/L_T}, \quad \text{where} \quad (9)$$

$$\delta T = T - T_{\text{eq}},$$

$$\delta T_0 = T_0 - T_{\text{eq}}, \quad (10)$$

$$T_{\text{eq}} = \frac{L_E T_{\text{AIR}} + L_A T_{\text{INT}}}{L_E + L_A} = \frac{T_{\text{AIR}} + T_{\text{INT}} \frac{M}{R\gamma_A}}{1 + \frac{M}{R\gamma_A}}, \quad \text{and} \quad (11)$$

$$L_T = \frac{L_E L_A}{L_E + L_A} = \frac{Q}{M + R\gamma_A}. \quad (12)$$

As for salinity, Eq. (9) describes an exponential adjustment of the inflow temperature toward an equilibrium value, T_{eq} , on the length scale L_T . The equilibrium temperature is the value that would be obtained if the boundary current were infinitely long and fully adjusted to the forcing. It is an average of T_{AIR} and T_{INT} , weighted by their exchange efficiency parameters. If the ratio of atmospheric forcing to exchange with the interior $R\gamma_A/M \ll 1$, then the interior dominates and $T_{\text{eq}} \approx T_{\text{INT}}$. When $R\gamma_A/M \gg 1$, then $T_{\text{eq}} \approx T_{\text{AIR}}$ and the atmosphere dominates the forcing.

F4 AU2 Figure 4 shows $T_{\text{eq}}/T_{\text{INT}}$ as a function of $R\gamma_A/M$, together with $S_{\text{EQ}}/S_{\text{INT}}$ as a function of F/M , and illustrates a key difference between the temperature and freshwater forcing: whereas S_{EQ} can take any value between 0 and S_{INT} , T_{eq} is constrained to the comparatively narrow interval $[T_{\text{INT}}, T_{\text{AIR}}]$ because the atmospheric heat

flux depends on the temperature of the water and approaches zero as $T \rightarrow T_{\text{AIR}}$.

The length scale L_T on which the temperature adjusts to T_{eq} is shorter than both the atmospheric adjustment length scale L_A and the interior adjustment length scale L_E . The ratio L_B/L_T determines the extent to which the boundary current has adjusted to the forcing when it exits the basin. Full adjustment (i.e., $T_{\text{OUT}} = T_{\text{eq}}$) occurs for $L_B/L_T \gg 1$. For $L_B/L_T < 1$ the outflow temperature also depends on the inflow temperature T_0 . As for the analogous salinity adjustment, T_{OUT} is most sensitive to the volume transport of the boundary current at $Q = 0.5L_B(M + R\gamma_A)$, or $L_B/L_T = 2$. Regimes relevant to the Nordic Seas will be discussed in section 5.

AU3

3. The buoyancy budget

We are now in a position to consider the buoyancy budget of the idealized current illustrated in Fig. 1. Assuming that density can be described by a linear equation of state—that is,

$$\rho(S, T) = \rho_0(1 + \beta S - \alpha T), \quad (13)$$

where $\rho_0 = 1000 \text{ kg m}^{-3}$ is a reference density, $\beta = 8 \times 10^{-4} \text{ psu}^{-1}$, and $\alpha = 2 \times 10^{-4} \text{ }^\circ\text{C}^{-1}$ —then from Eqs. (4) and (9) the normalized density anomaly $B(y)$ is given by

$$B(y) = \frac{\rho(y) - \rho_0}{\rho_0} = \beta(S_{\text{EQ}} + \delta S_0 e^{-y/L_S}) - \alpha(T_{\text{eq}} + \delta T_0 e^{-y/L_T}). \quad (14)$$

Figure 5 shows $\rho_0 B(y)$ for $S_{\text{EQ}} = 34 \text{ psu}$, $T_{\text{eq}} = 4^\circ\text{C}$, $L_F = 4000 \text{ km}$, $L_T = 1350 \text{ km}$, and four different combinations of initial temperature and salinity. In all four cases we have

$$\lim_{y \rightarrow \infty} B(y) = \beta S_{\text{EQ}} - \alpha T_{\text{eq}}; \quad (15)$$

that is, the density of the boundary current approaches an equilibrium value that is independent of Q and of the

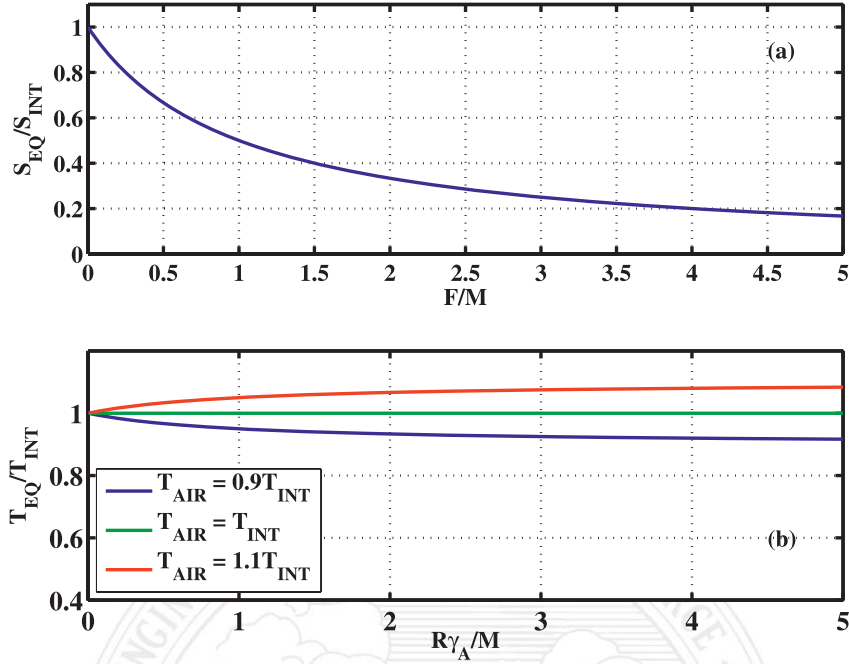


FIG. 4. (a) The equilibrium salinity divided by the interior salinity S_{EQ}/S_{INT} as a function of F/M , the ratio of the freshwater flux F to the rate at which the boundary current exchanges fluid with the basin interior, M . (b) The equilibrium temperature divided by the interior temperature T_{EQ}/T_{INT} as a function of $R\gamma_A/M$, the ratio of the atmospheric heat exchange, $R\gamma_A$, to the rate at which the boundary current exchanges fluid with the basin interior M . Three different values of the air temperature T_{AIR} are shown.

inflow values S_0 and T_0 . However, the two exponential functions in Eq. (14) lead to four possible regimes in which the density (i) increases monotonically, (ii) decreases monotonically, (iii) reaches a local maximum, or (iv) reaches a local minimum before arriving at the value (15). If the initial deviations, δT_0 and δS_0 , in temperature and salinity from their equilibrium values are of opposite sign, then the density change will be monotonic, with the boundary current either cooling and getting saltier, or warming and freshening, throughout the basin. However, if δT_0 and δS_0 are of the same sign, then the effects of temperature and salinity will oppose each other. For the case shown in Fig. 5 we have $L_T < L_S$; that is, the temperature adjusts faster than the salinity. Then the density change is initially governed by the temperature adjustment, followed by a more gradual change due to the salinity adjustment. If, however, $L_T > L_S$, then the salinity adjustment will dominate the density initially.

Because the density adjustment is governed by the initial deviations of salinity and temperature from their equilibrium values and the relative size of the adjustment length scales for salinity and temperature, the many parameters introduced in section 2 can be reduced to two key nondimensional parameters as follows. The

densification of the boundary current along its path, ΔB , is the difference in density between the inflow and the boundary current at any point y and is given by

$$\Delta B(y) \equiv B(y) - B(0) = \beta \delta S_0 (e^{-y/L_S} - 1) - \alpha \delta T_0 (e^{-y/L_T} - 1). \quad (16)$$

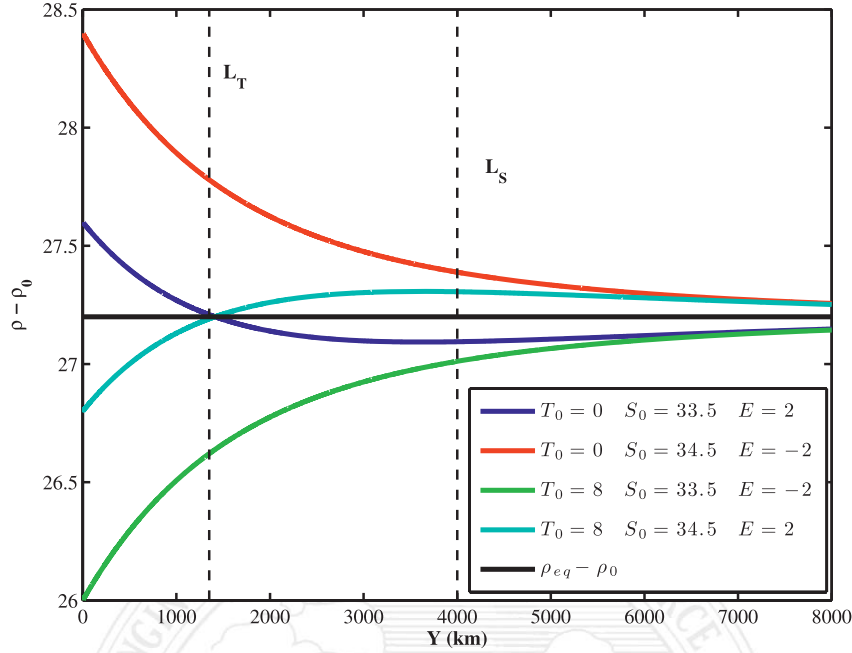
Dividing through by $\beta \delta S_0$, we obtain

$$\Delta \hat{B} = e^{-\hat{y}} - 1 - E(e^{-\hat{y}/\eta} - 1), \quad (17)$$

where

$$\begin{aligned} \Delta \hat{B} &= \frac{B(y) - B(0)}{\beta \delta S_0}, \\ E &= \frac{\alpha \delta T_0}{\beta \delta S_0}, \\ \eta &= \frac{L_T}{L_S} = \frac{F + M}{R\gamma_A + M}, \\ \hat{y} &= \frac{y}{L_S}, \end{aligned} \quad (18)$$

and $\hat{L}_B = L_B/L_S$.



AU14

FIG. 5. Density anomaly as a function of distance along the boundary current for $S_{eq} = 34$ psu, $T_{eq} = 4^\circ\text{C}$, $L_S = 4000$ km, and $L_T = 1350$ km and for four different combinations of inflow temperature and salinity.

The nondimensional density difference $\Delta\hat{B}$ is a function of only the two parameters, E and η . The sign of E determines whether the temperature and salinity adjustments have opposing or reinforcing effects on the density, and the magnitude of E describes the relative importance of temperature adjustment compared to salinity adjustment for the density. When $|E| > 1$ the initial temperature deviation from equilibrium has a larger impact on the density than the initial salinity deviation, and when $|E| < 1$ the initial salinity deviation has a larger impact than the temperature.

The parameter η is the ratio of the two adjustment length scales L_T and L_S . This depends only on the relative strength of the exchanges with the atmosphere and the basin interior. If there is no exchange with the interior, then $M = 0$ and $\eta = F/R\gamma_A$. If, on the other hand, the exchange with the interior dominates, then $M \gg F$, $M \gg R\gamma_A$, and $\eta \rightarrow 1$, since in the absence of atmospheric forcing both salinity and temperature will adjust on the same length scale. For the Nordic Seas parameter ranges considered in section 5, $F/R\gamma_A \ll 1$ and hence $0 < \eta < 1$, reflecting the fact that when only atmospheric forcing is considered, the temperature of the boundary current adjusts faster than its salinity.

The evolution of the nondimensional density difference $\Delta\hat{B}$ as the current flows around the basin is shown for different values of E and η in Fig. 6. Thin white lines

show $\Delta\hat{B}(\hat{y})$, and the background color indicates the value of η . For any given \hat{y} , $\Delta\hat{B}$ varies monotonically with η and lies within the range of values bounded by the two solutions $\Delta\hat{B}_{MIN}$ and $\Delta\hat{B}_{MAX}$, where

$$\begin{aligned} \Delta\hat{B}_{MIN} &= \lim_{\eta \rightarrow \infty} \Delta\hat{B}(\hat{y}) = e^{-\hat{y}} - 1, \\ \Delta\hat{B}_{MAX} &= \lim_{\eta \rightarrow 0} \Delta\hat{B}(\hat{y}) = e^{-\hat{y}} - 1 + E. \end{aligned} \quad (19)$$

The maximum and minimum values (19) are shown in Fig. 6 as black dashed lines. The six panels correspond to six different values of E , starting at $E = -3$ and then increasing to $E = 10$ in the last panel. The first two panels have negative E ; that is, the effects of temperature and salinity adjustment on the density reinforce each other, and so $\Delta\hat{B}$ decreases monotonically with \hat{y} from 0 to $E - 1$ for all η . Depending on the sign of δS_0 (and δT_0) these solutions correspond to a monotonically increasing or monotonically decreasing density.

The special case $E = 0$ (not shown) corresponds to the inflow temperature being equal to the equilibrium temperature T_{eq} , and therefore only salinity plays a role in the density adjustment. Analogously, when $E \rightarrow \infty$ the inflow salinity is equal to the equilibrium salinity and the density change is entirely governed by the temperature adjustment.

F6

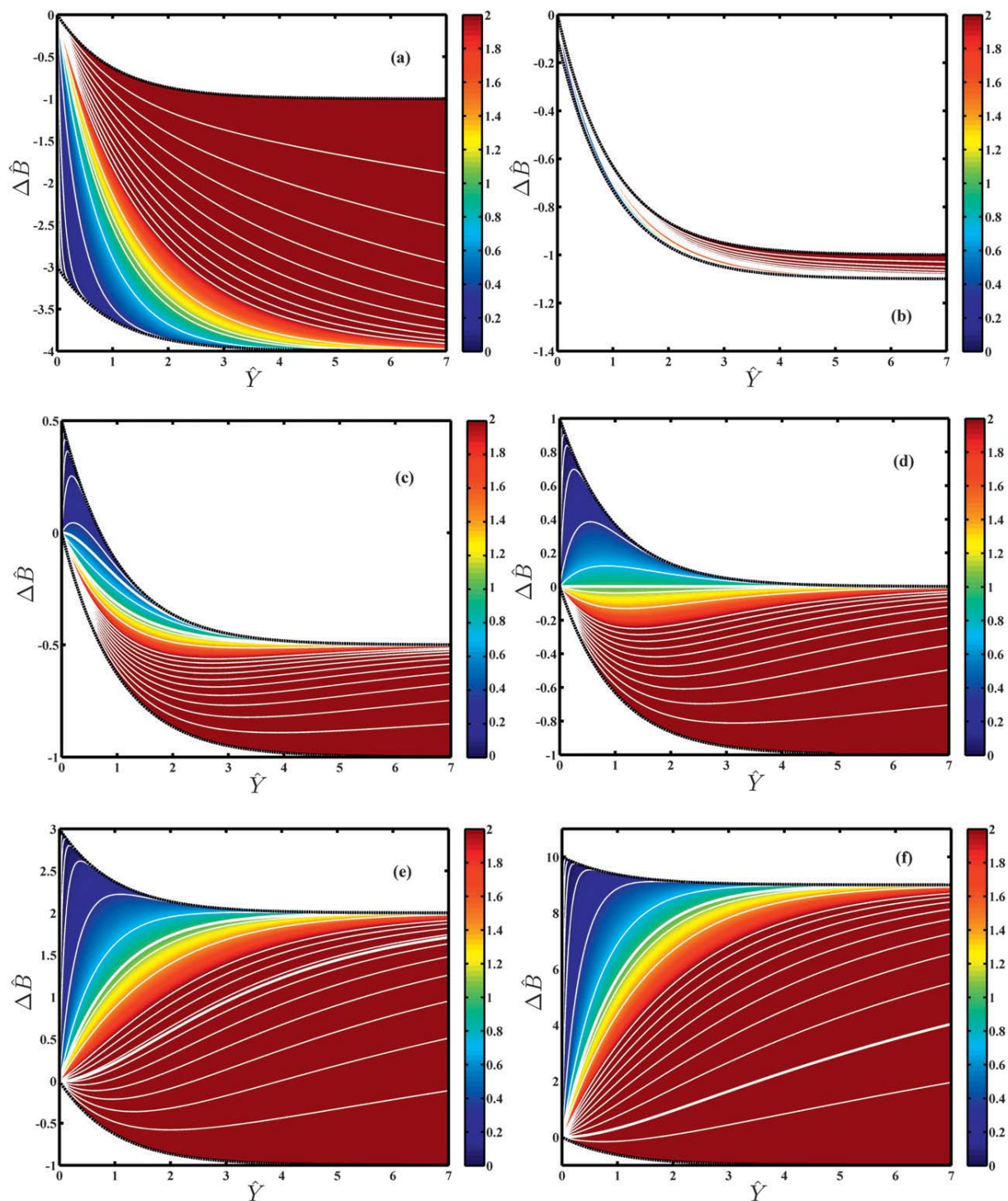


FIG. 6. The density difference between the boundary current and the inflow $\Delta\hat{B}$ as a function of η and \hat{y} for six different values of E . Thin white lines show different solutions, and the background colors indicate values of η according to the legend. The thicker white lines at $\eta = 1$ and $\eta = E$ indicate the boundaries between the regimes identified in the text.

For $E > 0$ (Figs. 6c–f) the four regimes illustrated in Fig. 5 are apparent, in which $\Delta\hat{B}$ increases to a local maximum, decreases to a local minimum, increases monotonically (only occurs for $E > 1$), or decreases monotonically (only occurs for $0 < E < 1$). Differentiating (17) with respect to \hat{y} gives

$$\frac{\partial\Delta\hat{B}}{\partial\hat{y}} = -e^{-\hat{y}} + \frac{E}{\eta}e^{-\hat{y}/\eta}, \quad (20)$$

which can only become zero if η has a value that does not lie between 1 and E . The limiting solutions for each regime are hence shown by the thick white lines drawn at $\eta = 1$ and $\eta = E$. For $E = 1$ (Fig. 6d) these lines collapse onto each other such that when $\eta < 1$ a local maximum in $\Delta\hat{B}$ is reached, whereas when $\eta > 1$ a local minimum is reached. All curves in all panels start at $\Delta\hat{B}(0) = 0$, although this is not always clear in Fig. 6 because of the abrupt initial change in density when $\eta \rightarrow 0$ (i.e., immediate temperature equilibration).

The density difference between the inflow and the outflow (i.e., the net densification within the marginal sea) is given by $\Delta\hat{B}(\hat{L}_B)$ and is shown in Fig. 7. It is clear from this and from expression (17) that when $E = 1$ and $\eta = 1$ there is no net density change within the basin ($\Delta\hat{B} = 0$), no matter what its size. Figure 6d shows that this is also the region of parameter space in which there are only two regimes, with density reaching either a local maximum or local minimum before it is fully adjusted. Hence, basins with $E \approx 1$ and $\eta \approx 1$ are particularly sensitive and small changes in the initial conditions or exchange parameters may alter the sign of the density change within the basin (i.e., switch from an outflow that is more buoyant than the inflow to one that is denser). For example, consider the case in which $\eta = 1$ and $\hat{L}_B = 0.5$ (and $\delta S_0 > 0$). If $E = 1.1$ the boundary current experiences a net increase in density during its journey through the basin, and, if the inflow is representative of the water in the open ocean outside, we might expect it to sink upon exit. However, if the temperature of the inflow were to decrease (or the salinity increase) such that E decreased to 0.9, the boundary current would become lighter during its transit through the basin and no longer sink upon exit. A similar regime change could be induced by increasing the freshwater forcing (and hence changing η).

When the density of the boundary current goes through a local maximum before adjustment, the outflow from the basin can be denser than the equilibrium value if the boundary current exits before it is fully equilibrated. This means that a denser outflow is possible when the surface buoyancy forcing is split between two components than when it is represented by only one component.

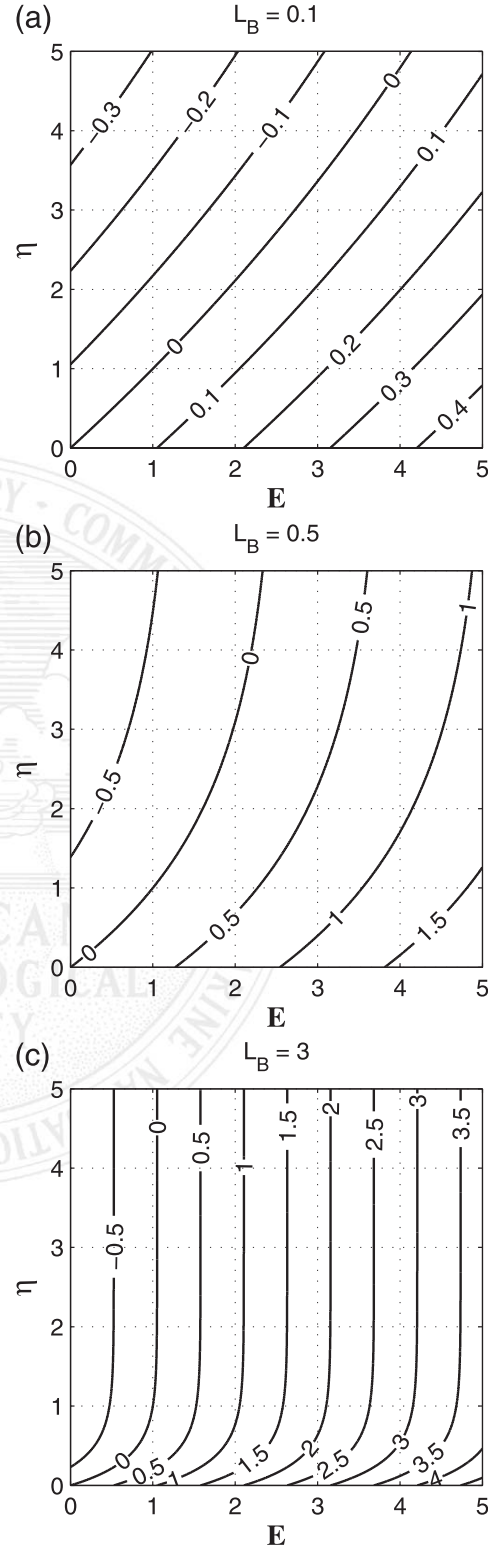


FIG. 7. Buoyancy change between the inflowing and outflowing boundary current $\Delta\hat{B}(\hat{L}_B)$ as a function of E and η for (a) $\hat{L}_B = 0.1$, (b) $\hat{L}_B = 0.5$, and (c) $\hat{L}_B = 3$.

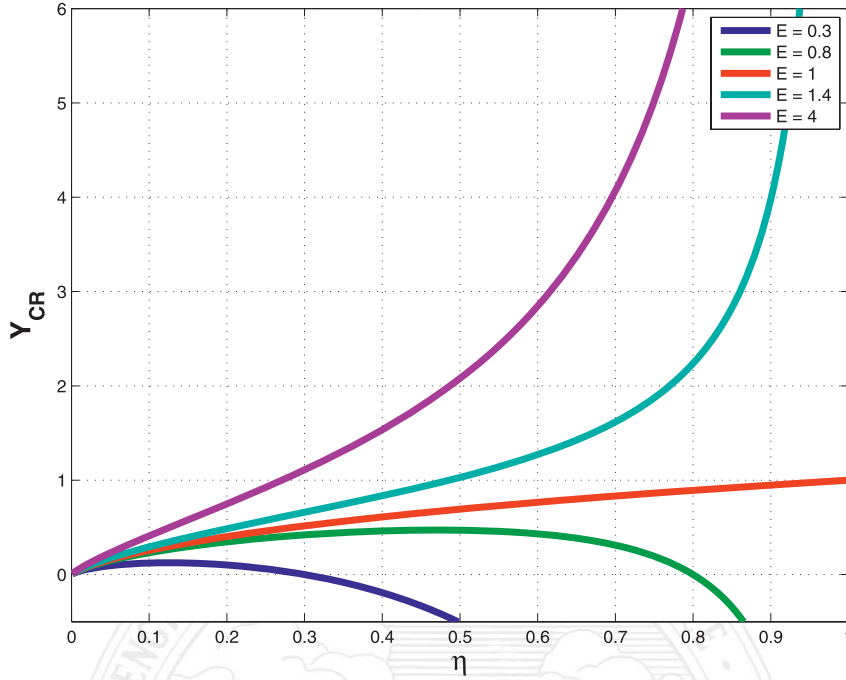


FIG. 8. Position \hat{y}_{cr} at which a boundary current density maximum or minimum occurs, as a function of η , for different values of E .

The density maximum will be studied in some detail in the following section.

4. Density maximum

The point of a local extremum in density, $\hat{y} = \hat{Y}_{CR}$, can be found using (20) and setting $d\Delta\hat{B}/d\hat{y} = 0$:

$$\hat{Y}_{CR}(\eta, E) = \frac{\eta}{1 - \eta} \ln\left(\frac{E}{\eta}\right). \quad (21)$$

F8 In Fig. 8, \hat{Y}_{CR} has been plotted as a function of η for five different values of E . Positive \hat{Y}_{CR} and a density maximum (i.e., $\partial^2\Delta\hat{B}/\partial\hat{y}^2 < 0$) require that

$$E > 0, \quad (22)$$

that is, that the temperature and salinity adjustments are acting in opposition (which for $F > 0$ means cooling and freshening) and that η falls in the range

$$0 < \eta < \min(E, 1). \quad (23)$$

Hence, the first requirement for an initially warm and salty boundary current to have a local maximum in density is that the temperature relaxation is faster than the salinity relaxation ($\eta < 1$). If the initial temperature deviation has a smaller effect on the density than the

salinity deviation ($E < 1$), then the temperature relaxation needs to be even faster ($\eta < E$). Furthermore, it is required that $\hat{L}_B > \hat{Y}_{CR}$ (i.e., that the basin is sufficiently large for the density maximum to fall within the marginal sea).

Substituting expression (21) for \hat{Y}_{CR} into the density Eq. (14) gives (after division by $\beta\delta S_0$) the value for \hat{B} at the local maximum,

$$\hat{B}_{MAX} = (1 - \eta) \left(\frac{E}{\eta}\right)^{\eta/\eta-1} + \hat{B}_{EQ}, \quad (24)$$

where

$$\hat{B}_{EQ} = \frac{\beta S_{EQ} - \alpha T_{EQ}}{\beta\delta S_0}.$$

Because $0 < \eta < \min(E, 1)$ according to (23) the singularity arising as $\eta \rightarrow 1^+$ is never approached. Figure 9 shows $\hat{B}(\hat{y}) - \hat{B}_{EQ}$ for $E = 0.8$ (green lines) and $E = 1.5$ (blue lines), and several different values of η ranging from 0.01 to 5. The local maximum points, given by (21) and (24), are shown as black dots. **F9**

For a fully adjusted basin, the maximum density reached by the boundary current is \hat{B}_{MAX} if there is a local maximum (black dots in Fig. 9) or, if E and η are not within the critical ranges given by (22) and (23), it is

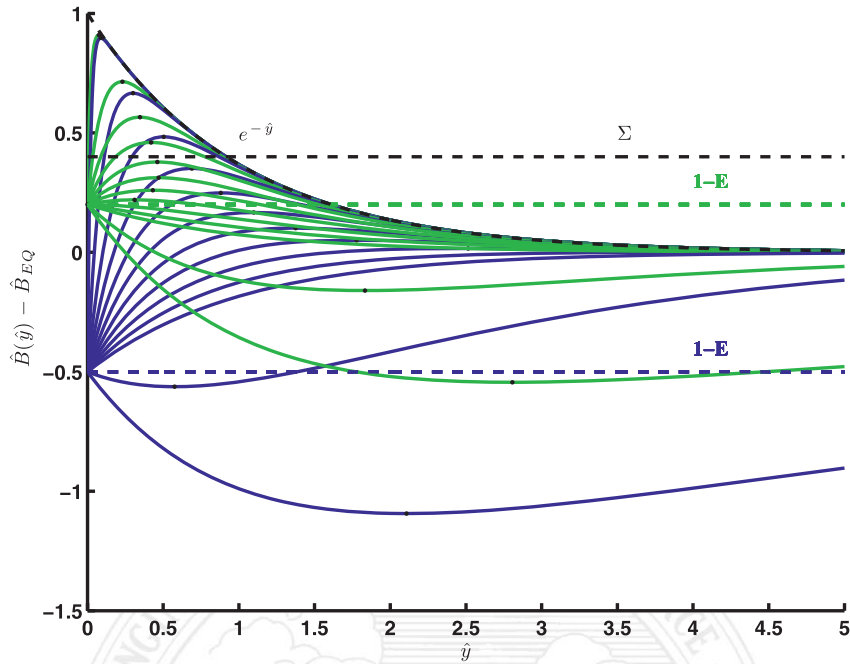


FIG. 9. The difference in density between the boundary current and its equilibrium value as a function of \hat{y} for $E = 0.8$ (green lines), $E = 1.5$ (blue lines), and increasing values of η ranging from 0.01 (uppermost curves) to 5 (lowermost curves). Local extreme values are shown by black dots. The dashed black line shows an arbitrary value of $\Sigma = 0.4$.

F10 the equilibrium density \hat{B}_{EQ} (if $E > 1$) or the initial value $\hat{B}(0) = 1 - E + \hat{B}_{EQ}$ (if $E < 1$). This maximum density (relative to the equilibrium density) is plotted in Fig. 10 as a function of η for different E .¹ It is clear from Fig. 10 and expression (24) that $\hat{B}_{MAX} - \hat{B}_{EQ}$ obtains its largest value of 1 for $\eta = 0$ (i.e., immediate temperature adjustment).

In a marginal sea with $F \geq 0$, the equilibrium density will always be lighter than or equal to the basin interior density. In a system in which density depends only on temperature (e.g., Spall 2004; Walin et al. 2004; Straneo 2006), or if the length scales for salinity and temperature adjustment are equal, the density will approach this equilibrium value monotonically and, since the current is buoyant when it enters the basin, it will remain buoyant during the adjustment. However, if we are in a region of parameter space in which the boundary current density reaches a local maximum before it decreases to the equilibrium value, then the boundary current can become denser than the basin interior and sink. Subduction points like this are present, for exam-

ple, in the Arctic Ocean (e.g., Saloranta and Haugan 2004) and affect the local climate since beyond this point there is no heat flux from the boundary current to the atmosphere. The buoyancy adjustment after such a point is no longer governed by (17) (besides losing contact with the atmosphere, a significant change in M can be expected, since the stability characteristics may change and the wind-driven Ekman transport shuts down), but the expression can still be used to find the location at which subduction occurs. It is one of the key findings of the present paper that only when the surface boundary conditions for temperature and salinity are different is subduction of the boundary current possible.

Because the boundary current must be buoyant on entering the marginal sea, the range of E is restricted to

$$E > 1 - \Sigma, \quad (25)$$

where Σ is the nondimensional density difference between the interior and the equilibrium value, given by

$$\Sigma = \frac{\rho_{INT} - \rho_{EQ}}{\rho_0 \beta \delta S_0}.$$

Restricting the analysis to basins for which $T_{INT} = T_{AIR}$ yields

¹ Note that for basins that satisfy conditions (22) and (23) but are not fully adjusted to the forcing (i.e., $\rho_{OUT} \neq \rho_{EQ}$), the maximum density will be less than \hat{B}_{MAX} if the local density maximum has not been reached before the current exits the basin.

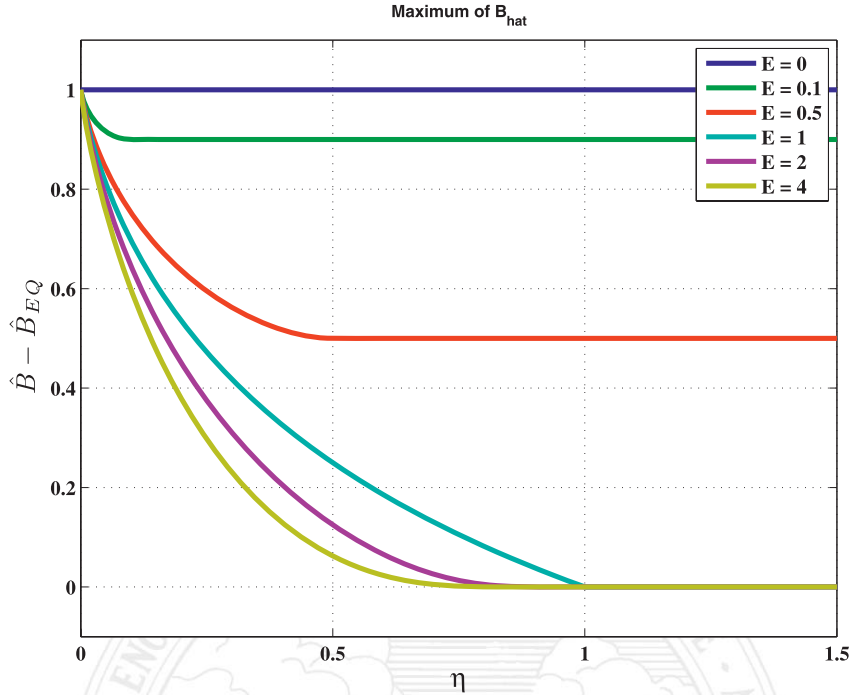


FIG. 10. The difference between the maximum density in the marginal sea and the equilibrium density, as a function of η , for some values of E . Note that this figure strictly applies only to those basins that are fully adjusted in terms of both temperature and salinity. The maximum density reached in other basins may be less than this.

$$\Sigma = \frac{S_{\text{INT}} - S_{\text{EQ}}}{\delta S_0} = \frac{FS_{\text{INT}}}{FS_0 + M(S_0 - S_{\text{INT}})}. \quad (26) \quad 0 < \Sigma < 1. \quad (28)$$

If the basin is sufficiently large that $\hat{L}_B \geq \hat{Y}_{\text{CR}}$, then subduction occurs if the density at the local maximum is greater than the interior density ($\rho_{\text{MAX}} > \rho_{\text{INT}}$) or equivalently, using (24), if

$$(1 - \eta) \left(\frac{E}{\eta} \right)^{\eta/\eta-1} > \Sigma.$$

Rearranging this expression and using the requirement (25) gives the range of E for which subduction occurs:

$$1 - \Sigma < E_{\text{SUB}} < \eta \left(\frac{\Sigma}{1 - \eta} \right)^{\eta-1/\eta}. \quad (27)$$

F11 The values of E given by (27) are shown in Fig. 11 as a function of η for three different values of Σ . The boundary current becomes denser than the interior and subducts in the shaded area of parameter space. Because subduction only occurs when there is a local maximum in density, the additional requirement on E_{SUB} is that it satisfy (22) and (23), both of which are true if

Using expressions (27) and (28), one can calculate whether the length scales of the basin (determining η and \hat{L}_B) permit subduction of the boundary current, and how warm and salty (determining E and Σ) the inflow must be for this to occur.

5. Application to the Nordic Seas

The simplified budget described so far is appropriate for any basin encircled by a boundary current that exchanges freshwater and heat with the atmosphere and basin interior. In this section we discuss the parameter ranges appropriate to the Nordic Seas and consider the extent to which the model is able to explain the properties of the outflow over the Greenland Scotland Ridge into the Atlantic.

A map of the surface temperature, salinity, and density of the Nordic Seas is shown in Isachsen et al. (2007, their Fig. 2). Figure 1 of the same paper shows the location of key geographical features in the region. Warm and relatively salty Atlantic water enters the Nordic Seas from the south as a buoyant coastal boundary current, and then cools and freshens as it travels cyclonically

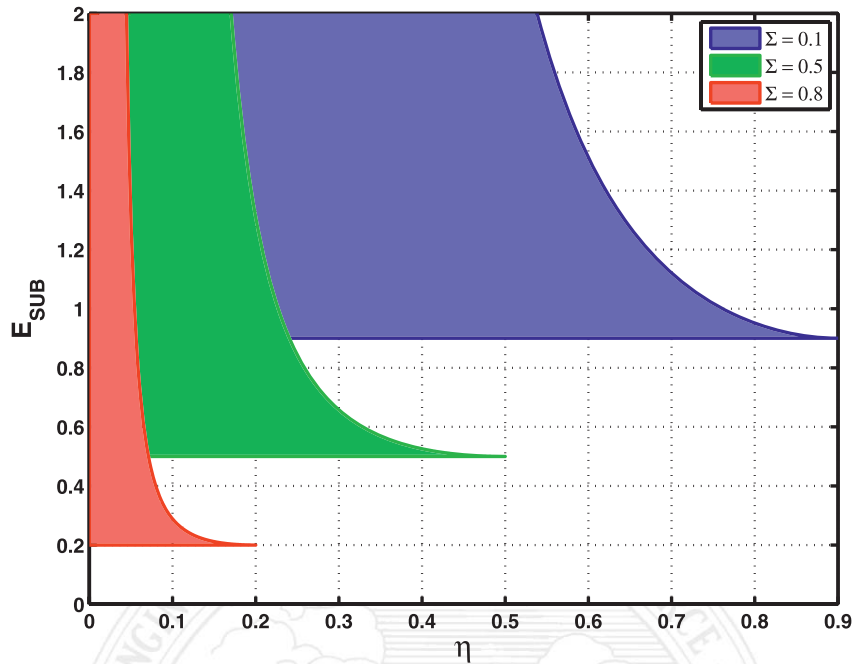


FIG. 11. The values of E for which subduction occurs within the basin, as a function of η (i.e., the ratio of the adjustment length scales for salinity and temperature), and for three different values of Σ (i.e., the nondimensional density difference between the interior and the equilibrium value). Subduction occurs for the combinations of E and η shown in the colored region provided the basin is sufficiently large for the local maximum in density to occur before the boundary current exits.

around the basin, steered by the bathymetry (Mauritzen 1996a,b). Both heat loss and the addition of freshwater have a significant effect on the boundary current density. The outflow from the Nordic Seas at Denmark Strait comprises dense overflow water as well as cold, fresh surface water over the Greenland shelf [see, e.g., Fig. 3 in chapter 19 of Dickson et al. (2008)]. The dense overflow water itself is stratified (although this is reduced during mixing in the overflow plume). In contrast, and by construction, the outflow from the model developed here occurs at a single density and can thus only be compared with the average properties of the overflow.

Parameters chosen to represent the Nordic Seas are listed in Table 1 and discussed in appendix B. All values are approximate, in keeping with the simplicity of the model, and uncertainty ranges are therefore not generally quoted. Midrange parameters lead to the following length scales: $L_S \sim 5100$ km, $L_E \sim 5300$ km, $L_A \sim 2500$ km, and $L_T \sim 1700$ km. For the Nordic Seas, therefore, $L_B \approx L_S \approx 3L_T$ and $L_T/L_A \approx 3/4$ —that is, the boundary current is not fully adjusted in terms of salinity, but almost adjusted in terms of temperature. Furthermore the atmosphere is more important than the basin interior for the temperature adjustment. Midrange values for F and M imply $S_{\text{eq}} = 33.6$ psu (with a range

of 32.6–34.0 psu), and $T_{\text{eq}} = T_{\text{AIR}} = T_{\text{INT}} = -0.5^\circ\text{C}$. Figures 12 and 13 illustrate the evolution of salinity and temperature around a hypothetical Nordic Seas basin, together with the outflow properties. It is clear from Fig. 12 that the range of possible values for the freshwater flux F has a bigger influence on the salinity than the uncertainty in M does. Note that any variation in air temperature around the basin has a negligible effect on the outflow (not shown) and is therefore not included here.

The dimensionless parameters governing the buoyancy adjustment of the Nordic Seas, for midrange values of the parameters in Table 1, are $E = 1.3$, $\eta = 0.34$, and $\hat{L}_B = 0.8$. Figure 14 shows the dimensionless density difference relative to the inflow $\Delta\hat{B}(\hat{y})$ [see Eq. (17)], as a function of E and η . The green dashed line corresponds to these midrange parameters, which give an increase of $\Delta\hat{B}(\hat{y})$ by 0.6 from inflow to outflow. This is equivalent to a densification of $\rho_0\beta\delta S_0\Delta\hat{B} = 0.8$ kg m⁻³ around the basin which, although subject to considerable uncertainty, agrees well with recent estimates made by Isachsen et al. (2007) of the isopycnal overturning north of the Greenland–Scotland Ridge (see their Fig. 12a).

The ranges of buoyancy parameters consistent with the values of F , M , and γ_A in Table 1 are $0.8 < E < 1.8$, $0.2 < \eta < 0.6$, and $0.5 < \hat{L}_B < 1.0$; Fig. 14 shows the

F12 F13

F14

T1

AU5

TABLE 1. Parameter values chosen for the Nordic Seas and the relevant references.

| Parameter | Nordic Seas value | Reference |
|---------------------------|---|--|
| L_B (m) | 4×10^6 | |
| Q (Sv) | 8 | Blindheim and Osterhus (2005) |
| R (m) | 2.5×10^5 | |
| S_{INT} (psu) | 34.9 | Blindheim and Osterhus (2005) |
| S_0 (psu) | 35.2 | Blindheim and Osterhus (2005) |
| T_{INT} ($^{\circ}C$) | -0.5 | Blindheim and Osterhus (2005) |
| T_{AIR} ($^{\circ}C$) | -0.5 | |
| T_0 ($^{\circ}C$) | 8.0 | Blindheim and Osterhus (2005) |
| F ($m^2 s^{-1}$) | 0.05-0.07 | Serreze et al. 2006, Dickson et al. 2007 |
| M ($m^2 s^{-1}$) | 1.0-2.0 | Furevik and Nilsen 2005, Iovino 2007, Spall 2004 |
| γ_A ($m s^{-1}$) | 5×10^{-6} - 2×10^{-5} | Gill (1986), Mauritzen et al. (1996x), Walin et al. (2004), Haney (1971) |

AU15

density evolution across this parameter space. Despite the uncertainty in $\Delta\hat{B}(\hat{L}_B)$ that results, and the stratified nature of the real outflow from the Nordic Seas (comprising water both lighter and denser than the inflow), some conclusions can nevertheless be drawn. The Nordic Seas boundary current lies in the sensitive region of parameter space where $E \sim 1$. This marks the boundary between different possible density regimes (see section 3). If $E < 1$ —consistent with the parameter ranges shown in Table 1, and illustrated by the blue lines in Fig. 14—then the equilibrium density is lighter than the inflow. A net densification only occurs because a local maximum in density is approached during the transit around the basin, and because the basin is not large enough to allow

complete adjustment to the forcing. This highlights several other important features of the Nordic Seas dense water formation process. First, the path length of the boundary current around the basin plays an important role. Although the path length itself is largely determined by topography (because the boundary current is constrained to flow along open geostrophic f/H contours), the relative path length compared to the basin adjustment length scales depends on the volume flux Q , as discussed in sections 2 and 3. Also, E , η , and $\Delta\hat{B}(\hat{y})$ are independent of Q , and so the effect of a change in boundary current strength on outflow density can be easily determined. A 20% weakening of the boundary current will result in a 25% increase in \hat{L}_B which,

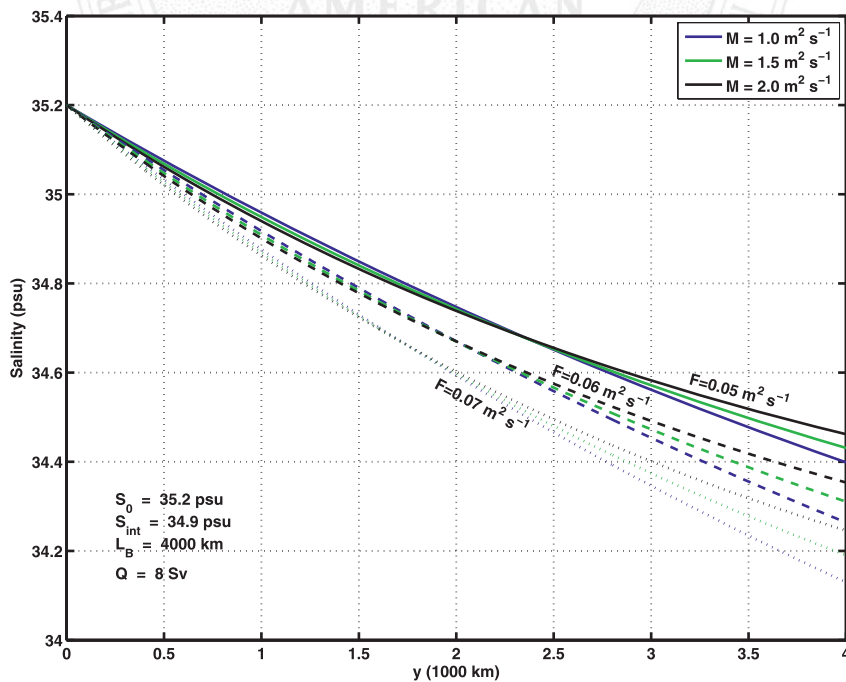


FIG. 12. Salinity as a function of y for parameters relevant to the Nordic Seas.

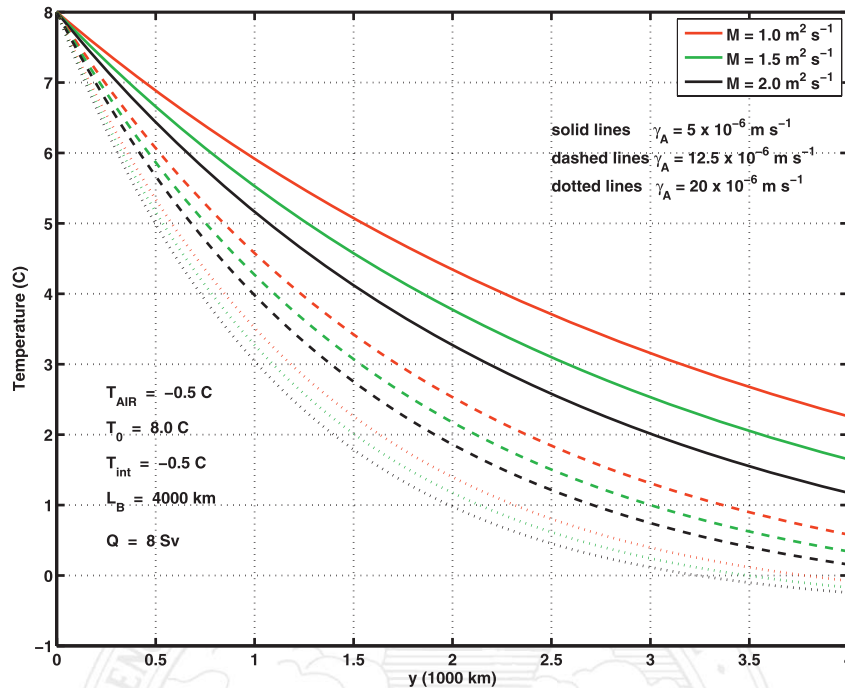


FIG. 13. Temperature as a function of y for parameters relevant to the Nordic Seas.

for some combinations of the parameters illustrated in Fig. 14, has a significant impact on the size (and even the sign) of the density change within the basin.

Second, because $\eta < 1$ and $\eta < E$, a local maximum in density is obtained before equilibration for all the parameter space shown, although this does not always occur within the basin. The boundary current is therefore not necessarily at its densest when it exits. There is also the potential for the boundary current to become denser than the interior and subduct beneath the surface. However, for the midrange parameters quoted, $\Sigma = 0.8$ and $E = 1.3$ which, according to Fig. 11, would require $\eta < 0.05$ for subduction to occur. Note that the present model does not explain the sinking of the Atlantic water in the proximity of Fram Strait, which is caused by the encounter there with the outflowing low-salinity polar water. In this simple model the freshwater added to the boundary current (including this outflow from the Arctic) is evenly distributed along its length, and only the vertical and cross-stream averaged properties of the boundary current are considered.

The sensitivity to each of the forcing parameters or initial conditions is readily assessed. For example, the freshwater flux F would have to be doubled for the boundary current to exit the basin lighter than it enters (assuming all other parameters remain unchanged). Increasing the density of the inflow (i.e., increasing S_0 or decreasing T_0) will result in less of a density change

during the transit through the basin (since the boundary current is approaching the same equilibrium density) but will nevertheless lead to a denser outflow, since this equilibrium density is not reached.

There are, of course, many caveats in applying a simplified model such as this to the Nordic Seas. In addition to the many basic assumptions outlined at the beginning of section 2 (including in particular the distribution of freshwater and interior exchange evenly around the basin and the assumption of a well-mixed boundary current in the vertical and cross-current directions), we have neglected the role of sea ice. Isachsen et al. (2007) find that this is responsible for less than 10% of the total densification within the region. We have also neglected the flow of Atlantic water into the Barents Sea, and one might argue that we should, rather, apply our simple model to the entire Arctic Mediterranean. The model implicitly assumes that the interior is convectively mixed down to at least sill depth, and the interior heat and buoyancy budgets demand that the basin must be significantly larger than the boundary current width to remain in steady state and for $T_{\text{INT}} \approx T_{\text{AIR}}$. We also make no attempt to allow for the seasonal cycle, although the transit through the basin takes 2–3 years. Nevertheless, the model does a credible job of representing the water mass transformation in the Nordic Seas and serves as a useful framework for thought experiments concerning the sensitivity of the system.

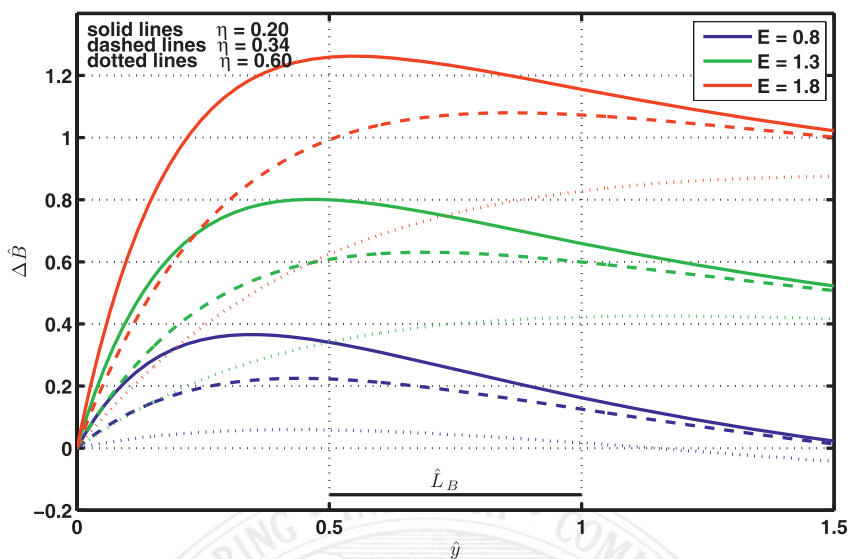


FIG. 14. Nondimensional density anomaly $\Delta\hat{B} = [B - B(0)]/\beta\delta S_0$ relative to the inflow for the parameter range appropriate to the Nordic Seas. The horizontal line at the bottom of the figure represents the range of reasonable values for the nondimensional boundary current length (i.e., the point that determines the outflow properties).

6. Discussion and conclusions

Previous model studies (e.g., Spall 2004; Walin et al. 2004) have shown that buoyancy loss over a marginal sea results in a buoyant coastal boundary current that flows cyclonically around the basin. Here, the heat, salt, and density budgets of such a boundary current have been presented. The conceptual model thus obtained differs from the one presented in Straneo (2006) in that (i) the effects of both temperature and salinity on density are considered and (ii) the boundary current interacts directly with the atmosphere, exchanging both heat and freshwater. The dynamics, however, are simplified compared to the Straneo (2006) study; most importantly, it is assumed that fluid is exchanged at a fixed rate between the boundary current and the basin interior, and the along-coast transport in the boundary current is assumed to be constant.

As the boundary current flows cyclonically around the basin, its temperature and salinity adjust in response to the surface (and terrestrial) forcing and to the exchange with the basin interior until it reaches an equilibrium salinity and temperature. The equilibrium values lie between the atmospheric values (i.e., $S = 0$ for salinity and $T = T_{ATM}$ for temperature) and the basin interior values. In general, however, temperature approaches its equilibrium value faster than salinity (i.e., temperature adjusts over a shorter length scale than salinity). The adjustment length scales for both heat (L_T) and salt (L_S) increase with the transport of the boundary current

and decrease with the strength of the exchange with the basin interior. However, L_S also decreases with the freshwater flux, whereas L_T decreases with the coefficient of temperature relaxation γ_A and the width of the current. The value of L_T obtained is supported by the experiments of Walin et al. (2004): the model developed here predicts a length scale of 1000 km based on Walin et al. (2004)'s parameters, which agrees roughly with their numerical results.

As a result of the two different adjustment length scales, the boundary current density can

- reach a value larger than that expected from the equivalent single-component density forcing because of the existence of a local maximum in density,
- become denser than the basin interior and subduct beneath the surface, and
- be sensitive to small changes in forcing parameters and boundary current path length, since these may induce a shift between different density adjustment regimes.

The outflow density in a marginal sea model using both salinity and temperature as forcings can therefore be quite different from a model that uses a single component to represent the equivalent buoyancy forcing. With a single component model, the density is constrained throughout to lie within the range bounded by the initial and equilibrium values.

Previous numerical and analytical studies of the buoyancy loss in horizontal gyres (e.g., Walin et al. 2004;

Spall 2004; Straneo 2006) have not been able to produce water that is denser than the water in the basin interior, and hence they cannot be reconciled with the conceptual picture of a marginal sea where light water enters, loses buoyancy, and sinks to the bottom before it exits again (e.g., Pratt and Whitehead 2008, chapters 2.13 and 2.14). The results presented in our section 4 illustrate that the effects of salinity and temperature must both be included to produce the maximum possible densification of the water flowing around a marginal sea. Maximum densification occurs when the length scale for temperature adjustment is short compared to that for salinity. In this case, a warm and salty inflow will lose most of its heat immediately upon entering the basin, whereas the salinity of the boundary current changes only slowly. Hence, the boundary current will quickly become denser because of the cooling. The density achieved when $L_T \rightarrow 0$ and $L_S \rightarrow \infty$ (i.e., when $R\gamma_A$ is large compared to M and F) can be thought of as the “densification potential” of the boundary current. Similarly, the most buoyant water a marginal sea can produce occurs when the boundary current freshens very quickly before any cooling has occurred.

Although the present model ceases to be valid when the current dives or subducts beneath the surface, it can be used to predict the point at which subduction occurs. It could also be used as a parameterization of the buoyancy changes that occur in a marginal sea. Given the bulk parameters $Q, F, M, R, L_B, S_{\text{INT}}, T_{\text{INT}}, T_{\text{AIR}}, \gamma_A, T_0$, and S_0 , the outflow properties can be calculated and fed back into a model of the neighboring ocean. For basins that are fully adjusted to their forcing, the outflow is furthermore independent of Q, T_0 , and S_0 .

The present results suggest that density increases within the Nordic Seas as a result of heat loss but that the boundary current is not fully adjusted with respect to salinity when it exits the basin. The outflow occurs close to a local maximum in density; if the boundary current were to follow a longer path, the density would decrease again because of salinity adjustment. In some plausible regions of parameter space the equilibrium density is, in fact, lighter than the inflow density, and it is only because the salinity adjustment occurs over length scales larger than the basin that a net densification occurs.

Acknowledgments. The authors are grateful to Fiamma Straneo and Tor Eldevik for organizing the Nordic Seas workshop at which we met, and which motivated this study. Both the Department of Meteorology at Stockholm University (MISU) and the Earth Sciences Centre at Gothenburg University provided travel funding for collaborative visits. We also thank Pal-Erik Isachsen and Cecilie Mauritzen for their useful feedback on an earlier draft. The comments of two anonymous re-

viewers helped to improve the manuscript significantly. HLJ is funded by a Royal Society University Research Fellowship, and AKW by the Swedish Research Council, for which we are grateful.

APPENDIX A

Title

AU6

Figure 3 shows a sketch of a small segment of the boundary current with length Δy and cross-sectional area A . A heat budget for the segment can be written as

$$\rho C_p \Delta y A \frac{\partial T}{\partial t} = \rho C_p Q T_1 - \rho C_p Q T_2 - \Delta y R q - \rho C_p M \Delta y (T - T_{\text{INT}}), \quad (\text{A1})$$

where ρ (kg m^{-3}) is the density, $C_p = 4200 \text{ J kg}^{-1} \text{ K}^{-1}$ is the heat capacity, t (s) is time, T_1 and T_2 are the temperatures of the water flowing into and out of the segment respectively, R is the width of the boundary current, q (W m^{-2}) is the heat flux to the atmosphere, and T_{INT} is the basin interior temperature. Assume now that the surface heat flux is proportional to the temperature difference between the ocean surface and the air, that is,

$$q = k(T - T_{\text{AIR}}). \quad (\text{A2})$$

Then (A1) can be written as

$$\Delta y A \frac{\partial T}{\partial t} = Q T_1 - Q T_2 - \Delta y R \gamma_A (T - T_{\text{AIR}}) - M \Delta y (T - T_{\text{INT}}), \quad (\text{A3})$$

where $\gamma_A = k/\rho C_p$ (m s^{-1}) is the temperature relaxation coefficient [see Haney (1971) and Wåhlin et al. (2009, manuscript submitted to *J. Fluid Mech.*)] for a discussion of its magnitude and relevance for a buoyancy-driven circulation). Dividing through by Δy , we find that in steady state, and in the limit $\Delta y \rightarrow 0$, (A3) reduces to

$$Q \frac{dT}{dy} = -R \gamma_A (T - T_{\text{AIR}}) - M (T - T_{\text{INT}}),$$

that is, to expression (6).

APPENDIX B

Title

AU7

The estimates of Nordic Seas parameters given in Table 1 are approximate and uncertainty values are therefore

not generally quoted. Values for the inflow and basin interior properties are based on Blindheim and Osterhus (2005) and Nilsen (xxxx, personal communication), and the atmospheric temperature to which the boundary current relaxes is taken to be $T_{\text{AIR}} = T_{\text{INT}}$ since the interior of the basin is presumably in equilibrium with the atmosphere. We consider a likely range for F of $0.05\text{--}0.07\text{ m}^2\text{ s}^{-1}$. This is roughly in keeping with an input of 0.15 Sv ($1\text{ Sv} \equiv 10^6\text{ m}^3\text{ s}^{-1}$) from the Arctic via Fram Strait and up to 0.1 Sv from the Norwegian coast, North Sea, and Greenland and precipitation minus evaporation (Serreze et al. 2006; Dickson et al. 2007). Note that runoff from northern Europe is actually delivered to the boundary current through exchange with the Norwegian coastal current onshore. While there is a large evaporative loss over the Atlantic inflow, this and other coastal runoff, together with precipitation, results in a positive freshwater flux. The total amount of freshwater added to the Nordic Seas basin is small compared to the volume flux of the boundary current (8 Sv).

The exchange with the interior is comprised of Ekman (M_{EK}) and eddy (M_{EDDY}) transports: M_{EK} is approximately $0.5\text{--}1.0\text{ m}^2\text{ s}^{-1}$ (Furevik and Nilsen 2005) and an upper estimate of M_{EDDY} can be obtained from a heat budget for the Greenland Sea as in Iovino (2007), which gives M_{EDDY} around $0.8\text{ m}^2\text{ s}^{-1}$. Spall (2004) calculates an azimuthally averaged value for the eddy fluxes in numerical simulations performed with an idealized general circulation model. The maximum value obtained in that study equates to an M_{EDDY} of $0.6\text{ m}^2\text{ s}^{-1}$. Assuming that these very rough estimates of eddy exchange are representative of the boundary current throughout the Nordic Seas, we consider a total range for $M = M_{\text{EK}} + M_{\text{EDDY}}$ of $1.0\text{--}2.0\text{ m}^2\text{ s}^{-1}$. The fact that M is not dominated by the eddy exchange reduces the impact of our assumption that M is uniform with y and independent of the density gradient between boundary current and basin interior.

The temperature relaxation coefficient γ_A is perhaps the least well known of the parameters in Table 1. It can be estimated using the sensible heat flux formula in Gill (1986) as in most atmospheric and coupled climate models. Together with a mean wind speed of 10 m s^{-1} and the knowledge that the total heat flux over the Nordic Seas comprises roughly 40% sensible and 60% latent components (Furevik and Nilsen 2005), this gives a value of $5\text{--}10 \times 10^{-6}\text{ m s}^{-1}$. A similar range is obtained based on a climatological heat loss of $30\text{--}60\text{ W m}^{-2}$ (Mauritzen et al. 1996x) and an average air–sea temperature difference over the Nordic Seas of 2°C . These estimates are equivalent to mixing surface temperature anomalies over an 800-m-deep boundary current on a time scale of 2–4 yr. The global mean value quoted in

Haney (1971) is $8 \times 10^{-6}\text{ m s}^{-1}$. However, Walin et al. (2004) used a higher value of $2.3 \times 10^{-5}\text{ m s}^{-1}$, for which no further motivation was provided but which gave a realistic ocean response to the atmospheric forcing, and so we consider the range $5\text{--}20 \times 10^{-6}\text{ m s}^{-1}$.

REFERENCES

- Blindheim, J., and S. Osterhus, 2005: The Nordic Seas: Main oceanographic features. *The Nordic Seas: An Integrated Perspective*, *Geophys. Mongr.*, Vol. 158, Amer. Geophys. Union, 11–38.
- Cessi, P., 2008: An energy-constrained parameterization of eddy buoyancy flux. *J. Phys. Oceanogr.*, **38**, 1807–1819.
- Dickson, R., B. Rudels, S. Dye, M. Karcher, J. Meincke, and I. Yashayaev, 2007: Current estimates of freshwater flux through Arctic and subarctic seas. *Prog. Oceanogr.*, **73**, 210–230.
- , J. Meincke, and P. Rhines, Eds., 2008: *Arctic–Subarctic Ocean Fluxes: Defining the Role of the Northern Seas in Climate*. Springer, 736 pp.
- Furevik, T., and J. E. Ø. Nilsen, 2005: The large-scale atmospheric circulation variability and its impact in the Nordic Seas ocean climate: A review. *The Nordic Seas: An Integrated Perspective*, *Geophys. Mongr.*, Vol. 158, Amer. Geophys. Union, xx–xx.
- Gill, A., 1986: *Atmosphere–Ocean Dynamics*. Academic Press, 662 pp.
- Haney, R. L., 1971: Surface thermal boundary condition for ocean circulation models. *J. Phys. Oceanogr.*, **1**, 241–248.
- Iovino, D., 2007: On the Nordic Seas' role in the Atlantic meridional overturning circulation. Ph.D. thesis, University of Bergen, xxx pp.
- Isachsen, P. E., C. Mauritzen, and H. Svendsen, 2007: Dense water formation in the Nordic Seas diagnosed from sea surface buoyancy fluxes. *Deep-Sea Res. I*, **54**, 22–41.
- Mauritzen, C., 1996a: Production of dense overflow waters feeding the North Atlantic across the Greenland–Scotland Ridge. Part 1. Evidence for a revised circulation scheme. *Deep-Sea Res. I*, **43**, 769–806.
- , 1996b: Production of dense overflow waters feeding the North Atlantic across the Greenland–Scotland Ridge. Part 2. An inverse model. *Deep-Sea Res. I*, **43**, 807–835.
- Pratt, L., and J. Whitehead, 2008: *Rotating Hydraulics: Nonlinear Topographic Effects in the Ocean and the Atmosphere*. Springer, 589 pp.
- Saloranta, T. M., and P. M. Haugan, 2004: Northward cooling and freshening of the warm core of the West Spitsbergen Current. *Polar Res.*, **23**, 79–88.
- Serreze, M. C., and Coauthors, 2006: The large-scale freshwater cycle of the Arctic. *J. Geophys. Res.*, **111**, C11010, doi:10.1029/2005JC003424.
- Solomon, S., D. Qin, M. Manning, M. Marquis, K. Averyt, M. M. B. Tignor, H. L. Miller Jr., and Z. Chen, Eds., 2007: *Climate Change 2007: The Physical Science Basis*. Cambridge University Press, 996 pp.
- Spall, M., 2002: Wind- and buoyancy-forced upper ocean circulation in two-strait marginal seas with application to the Japan/East Sea. *J. Geophys. Res.*, **107**, 3006, doi:10.1029/2001JC000966.
- , 2003: On the thermohaline circulation in flat bottom marginal seas. *J. Mar. Res.*, **61**, 1–25.
- , 2004: Boundary currents and watermass transformation in marginal seas. *J. Phys. Oceanogr.*, **34**, 1197–1213.

AU10

AU11

AU9

- , and R. S. Pickart, 2001: Where does dense water sink? A subpolar gyre example *J. Phys. Oceanogr.*, **31**, 810–826. **AU12**
- Strano, F., 2006: On the connection between dense water formation, overturning, and poleward heat transport in a convective basin. *J. Phys. Oceanogr.*, **36**, 1822–1840.
- Vellinga, M., and R. Wood, 2002: Global climatic impacts of a collapse of the Atlantic thermohaline circulation. *Climatic Change*, **54**, 251–267.
- Wåhlin, A. K., M. Ericsson, E. Aas, G. Broström, J. E. Weber, and J. Grue, 2009: Horizontal convection in water heated by infrared radiation and cooled by evaporation: Experimental results and scaling analysis. *J. Fluid Mech.*, submitted. **AU13**
- Walín, G., G. Broström, J. Nilsson, and O. Dahl, 2004: Baroclinic boundary currents with downstream decreasing buoyancy: A study of an idealized Nordic Seas system. *J. Mar. Res.*, **62**, 517–543.

